

FINITE ELEMENT MODELING OF TREE COIL EDDY CURRENT TRANSDUCER

Maria WRZUSZCZAK, Janusz WRZUSZCZAK

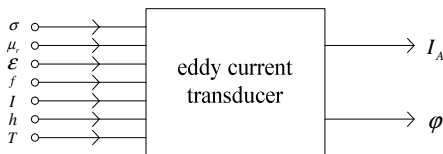
Opole University of Technology, Faculty of Electrical Engineering, Automatic Control and Informatics,
Sosnkowski Street 31, 45-232 Opole, Poland, tel.: 774498648, e-mail: m.wruszczak@po.opole.pl

Abstract: The paper deals with analysis of metrological properties of three-coil model of eddy current transducer. With finite element method (FEM) the distribution of electromagnetic fields for eddy current transducer model and various conducting materials such as metal and alloys without and with flaw has been presented. The real and imaginary part or magnitude and phase of induced current in output coils of the transducers models were calculated.

Keywords: modeling eddy current transducer, FEM.

1. INTRODUCTION

Non-destructive eddy current testing method is fast and effective for detecting and sizing most of the surface flaws in conducting materials. Small initial cracks on material surface that cannot be detected with ultrasonic testing, could be found with eddy current testing. This method can be applied to measure conductivity of conducting materials such as metal, alloys and semiconductors, and to thickness measurement of tubes wall [1, 2]. The amplitude and phase of the induced signal in output coil depends on several parameters e.g.: conductivity σ and relative magnetic permeability μ_r of materials of the testing object, electrical permittivity ε of sensor environment (air), frequency f and amplitude I of the excitation current, distance h between probe and specimen, temperature T , dimension of material flaws, properties such as discontinuity and non-homogeneity. Multi input - multi output model for eddy current transducer is shown in Fig.1.



Rys. 1. Multi input - multi output model of eddy current transducer, I_A, φ - magnitude and phase of output signal

The output signal I_2 from the transducer is a complex signal, its amplitude and phase, or real and imaginary part contain information about the measurand

$$I_2 = \text{Re}(I_2) + j\text{Im}(I_2) = I_A e^{j\varphi} \quad (1)$$

where

$$I_A = \sqrt{\text{Re}^2(I_2) + \text{Im}^2(I_2)} \quad (2)$$

$$\varphi = \arctg \frac{\text{Im}(I_2)}{\text{Re}(I_2)} \quad (3)$$

When the conductivity of material is the measurand, all other input parameter from model in Fig. 1 should have constant value.

2. MATHEMATICAL MODEL OF THE SENSOR WITH TESTING MATERIAL

The Maxwell's equations for eddy current transducer and conducting material have form

$$\nabla \times \vec{H}(x, y, z, t) = \vec{j}_e(x, y, z, t) + \frac{\partial \vec{D}(x, y, z, t)}{\partial t} \quad (4)$$

$$\nabla \times \vec{E}(x, y, z, t) = -\frac{\partial \vec{B}(x, y, z, t)}{\partial t} \quad (5)$$

$$\nabla \cdot \vec{B}(x, y, z, t) = 0 \quad (6)$$

$$\nabla \cdot \vec{D}(x, y, z, t) = \rho \quad (7)$$

$$\vec{D} = \varepsilon_0 \varepsilon_r \vec{E} + \vec{P} \quad (8)$$

$$\vec{B} = \mu_0 \mu_r (\vec{H} + \vec{M}) \quad (9)$$

where \vec{H} - magnetic field intensity, \vec{j}_e - current density in exciting coil, \vec{D} - electric displacement (electric flux density), \vec{E} - electric field intensity, \vec{B} - magnetic flux density, \vec{P} - electric polarization vector, \vec{M} - magnetization vector, ε_0 - permittivity of vacuum, ε_r - relative permittivity of material, μ_0 - permeability of vacuum, μ_r - relative permeability of material, ρ - electric charge density [2].

In cylindrical coordinates, for sinusoidal excitation current, the eddy current transducer together with testing material can be described for the magnetic potential vector \vec{A} with the Helmholtz equation

$$\nabla^2 A_\varphi + k^2 A_\varphi = -\mu_0 \mu_r j_{e\varphi} \quad (10)$$

$$k^2 = \omega^2 \mu \epsilon - j \omega \mu \sigma \quad (11)$$

$$\mu = \mu_0 \mu_r, \quad \epsilon = \epsilon_0 \epsilon_r \quad (12)$$

where $j_{e\varphi}$ azimuthal coordinate of current density in the exciting coil, A_φ azimuthal coordinate of magnetic potential vector. (In cylindrical coordinates is only one nonzero coordinate). For insulator (exemplary air) $k^2 = \omega^2 \mu \epsilon$ and for good conductor $k^2 = -j \omega \mu \sigma$. Equation (10) was the basic equation to calculate the electromagnetic field around eddy current sensor with FEM. For testing frequency satisfying condition $l \ll \lambda$ (where l - maximal dimension of testing object, λ - wavelength in vacuum) and $f \ll c/l$ (c - velocity of light propagation in vacuum), the problem can be solved as a quasistatic one [2].

3. FEM SIMULATION MODEL OF THREE – COIL EDDY CURRENT TRANSDUCER

Eddy current transducer can have different geometrical construction. Typically, they have one inductance coil for exciting the electromagnetic field and one or more output (measurement) coils [1-3]. In Fig. 2 is shown one of typical structure of eddy current transducer for metal surface testing.

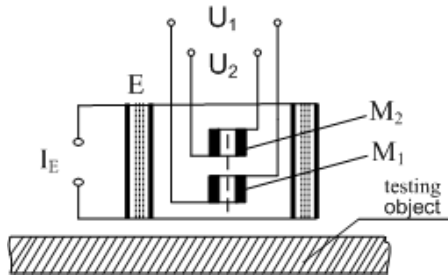


Fig. 2. Exemplary schematic diagram of eddy current transducer, E – exciting coil, M₁, M₂ – output coils

The FEM simulations were made with Comsol [3]. A simple axial symmetry model of the considered three - coil eddy current transducer from Fig. 2 over the testing material is shown in Fig. 3. It consists of one exciting coil E and two output coils M₁, M₂ each with 5 mm radius and 2 mm wire cross section diameters. The coil was fabricated from copper with conductivity $58 \cdot 10^6 \text{ S/m}$ and $\mu_r = 1$. For numerical simulations the conductivity of tested material was $\sigma = 35 \text{ MS/m}$ (aluminum) and relative permeability $\mu_r = 1$. The flaw in tested material is as circular discontinuity (material: air) with triangular cross section with depth $h = 3 \text{ mm}$ and width 2 mm. Thickness of the testing specimen is 10 mm. Current density in the exciting coil E $j_e = 10^6 \text{ A/m}^2$. The symmetry axis is at $r = 0$. The distribution of the magnetic flux density and eddy current density around three - coils transducer model is presented in Fig. 4.

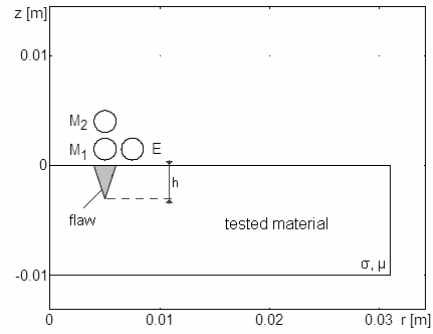


Fig. 3. Axial symmetry model for three-coils eddy current transducer and testing object (conducting material with flaw), E – exciting coil, M₁, M₂ – output coils; symmetry axis at $r = 0$, scale 1:1

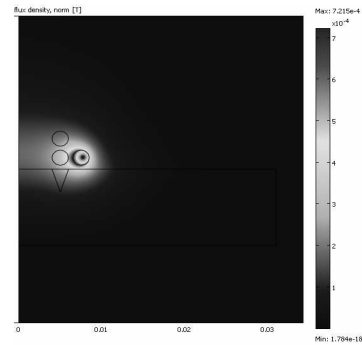


Fig. 4. Magnetic flux density B - modulus in T. Simulation results for model from Fig. 3 for aluminum with flaw, frequency $f = 500 \text{ Hz}$

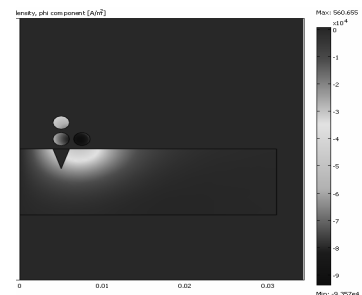


Fig. 5. Eddy current density j_φ in A/m^2 . Simulation results for model from Fig. 3 for aluminum with flaw; frequency $f = 500 \text{ Hz}$

Simulation for transducer model for flawless material and with flaw for frequency from range $5 \text{ Hz} \div 2 \cdot 10^5 \text{ Hz}$ has been performed. The induced currents in output coils M₁ and M₂ (output signals) is given by

$$I = \int_S j_\varphi dS \quad (13)$$

where: j_φ - eddy current density, dS - infinitesimal wire coil cross section.

Values of the induced current output signals are complex number, their real and imaginary part in coils M₁, M₂ versus frequency are presented in Fig. 6 and Fig.7 respectively.

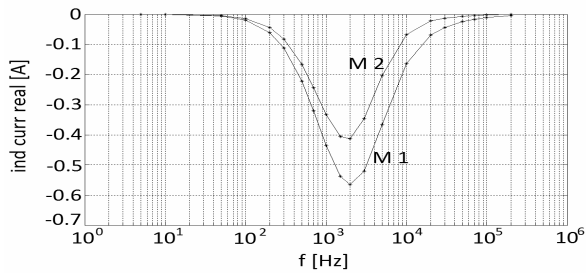


Fig. 6. Real part of induced current in output coils M_1 , M_2 versus frequency for flawless material

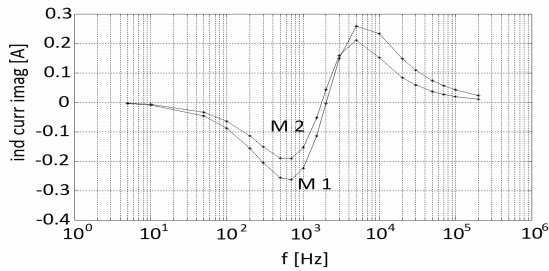


Fig. 7. Imaginary part of induced currents in output coils M_1 , M_2 versus frequency for flawless material

The magnitude and phase of induced current in coil M_1 , M_2 are shown in Fig. 8 and 9.

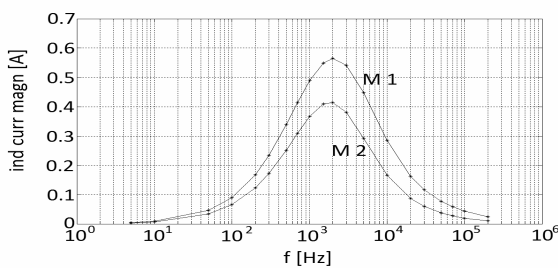


Fig. 8. Magnitude of induced currents in output coils M_1 , M_2 versus frequency for flawless material

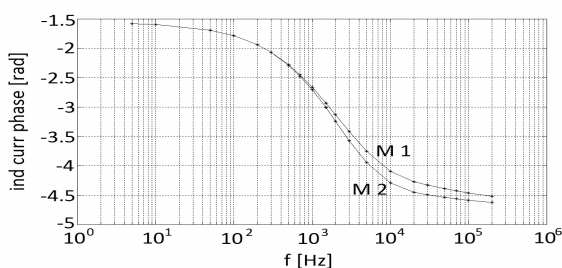


Fig. 9. Phase of induced currents in output coils M_1 , M_2 versus frequency for flawless material

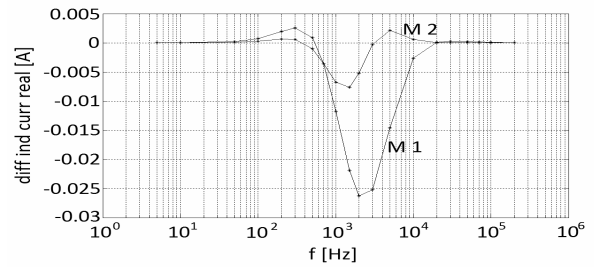


Fig. 10. Difference of induced current in output coils M_1 , M_2 (real part) for material with flaw and flawless materials versus frequency, circular flaw with triangular cross section (depth $h=3$ mm, width 2 mm)

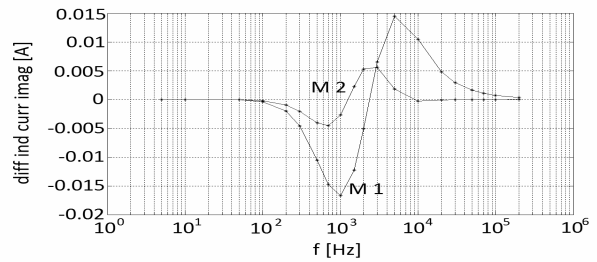


Fig. 11. Difference of induced current in output coils M_1 , M_2 (imaginary part) for material with flaw and flawless materials versus frequency, circular flaw with triangular cross section (depth $h=3$ mm, width 2 mm)

The output signal of induced current due to materials flaw has been calculated as a difference between simulation results for material with flaw and flawless material. The real and imaginary part of the flaw signals in coil M_1 , M_2 are presented in Fig. 10 and Fig. 11.

4. CONCLUSIONS

In the paper the methods of investigation metrological properties of eddy current transducers are presented. The simple models can give answer what influence have the material parameters and the size of flaw on the transducer output signal. We can also test the influence of the distance between transducer and investigated object on the output signals. The simulation results give practical suggestion for constructing new types of transducers. Eddy current transducers have various construction, but for most of them can be successfully simulated by presented model.

5. BIBLIOGRAFIA

1. Mc Master R., Mc Intire P.: Non Destructive Testing Handbook, Vol. 4, Electromagnetic Testing, (ASTM) Columbus, Ohio 1988.
2. Wrzuszczak M.: Modeling of Eddy Current Transducer, Politechnika Opolska, Studia i monografie, Opole 2011.
3. Comsol Multiphysics (www.comsol.com).

BADANIA SYMULACYJNE TRÓJCIEWKOWEGO PRZETWORNIKA WIROPRAĐOWEGO METODĄ ELEMENTÓW SKOŃCZONYCH

W pracy przedstawiono wyniki badań symulacyjnych metodą elementów skończonych dla trójcewkowego przetwornika wiroprowadowego stosowanego w defektoskopii wiroprowadowej. Przedstawiono rozkład modułu indukcji magnetycznej wokół modelu przetwornika nad przewodzącym materiałem z wadą oraz gęstości prądów wirowych w metalu. Obliczono wartości amplitudy i fazy prądu wyindukowanego w cewkach pomiarowych przetwornika. Wyniki badań uzyskane na prostym modelu można wykorzystać do analizy właściwości metrologicznych przetworników rzeczywistych.

Słowa kluczowe: modelowanie MES, przetworniki wiroprowadowe, przetwornik trójcewkowy.